Biocompatible Label-Free Detection of Carbon Black Particles by Femtosecond Pulsed Laser Microscopy

Peer-reviewed author version

BOVE, Hannelore; Steuwe, Christian; Fron, Eduard; SLENDERS, Eli; D'HAEN, Jan; Fujita, Yasuhiko; Uji-i, Hiroshi; VAN DE VEN, Martin; Roeffaers, Maarten & AMELOOT, Marcel (2016) Biocompatible Label-Free Detection of Carbon Black Particles by Femtosecond Pulsed Laser Microscopy. In: NANO LETTERS, 16 (5), p. 3173-3178.

DOI: 10.1021/acs.nanolett.6b00502
Handle: http://hdl.handle.net/1942/21558

Biocompatible Label-free Detection of Carbon Black Particles by Femtosecond Pulsed Laser Microscopy

Hannelore Bové[‡1,2], Christian Steuwe[‡2], Eduard Fron[3], Eli Slenders[1], Jan D'Haen[4], Yasuhiko Fujita[3], Hiroshi Uji-i[3,5], Martin vandeVen[1], Maarten Roeffaers[2], and Marcel Ameloot[1*]*

[1] Biomedical Research Institute, Hasselt University, Agoralaan Building C, 3590 Diepenbeek, Belgium

[2] Centre for Surface Chemistry and Catalysis, KU Leuven, Celestijnenlaan 200F, 3001 Leuven, Belgium

[3] Department of Chemistry, KU Leuven, Celestijnenlaan 200F, 3001 Leuven, Belgium

[4] Institute for Material Research, Hasselt University, Wetenschapspark 1, 3950 Diepenbeek, Belgium

[5] Research Institute for Electronic Science, Hokkaido University, N20W10, Kita-Ward Sapporo 001-0020, Japan

[‡] These authors contributed equally to this work

[*] maarten.roeffaers@biw.kuleuven.be and marcel.ameloot@uhasselt.be

KEYWORDS: Carbon black particles, label-free detection in aqueous environments, white light emission, femtosecond pulsed laser illumination, human lung fibroblasts.

ABSTRACT While adverse health effects of carbon black (CB) exposure are generally accepted, a direct, label-free approach for detecting CB particles in fluids and at the cellular level is still lacking. Here, we report non-incandescence related white-light (WL) generation by dry and suspended carbon black particles under illumination with femtosecond (fs) pulsed near-infrared light as a powerful tool for the detection of these carbonaceous materials. This observation is done for four different CB species with diameters ranging from 13 to 500 nm, suggesting this WL emission under fs near-infrared illumination is a general property of CB particles. As the emitted radiation spreads over the whole visible spectrum, detection is straightforward and flexible. The unique property of the described WL emission allows optical detection and unequivocal localization of CB particles in fluids and in cellular environments while simultaneously co-localizing different cellular components using various specific fluorophores as shown here using human lung fibroblasts. The experiments are performed on a typical multiphoton laser-scanning microscopy platform, widely available in research laboratories.

TEXT Carbon black (CB) consists of aciniform aggregates of primary particles with an elemental carbon content greater than 97 %.[1, 2] It is produced through well controlled incomplete combustion of organics like heavy petroleum or vegetable oil. This distinguishes CB from soot or black carbon, the unwanted by-product released during incomplete combustion processes such as in the exhausts of diesel engines and one of the main contributing factors to atmospheric particulate pollution.[2, 3] Nonetheless, due to the (physico)chemical similarity CB is widely used as a model compound for soot.[4, 5] The total global black carbon emission was estimated to be approximately 8.5 million tons after having constantly increased throughout the preceding decade.[6-8] As a consequence of the increasing

environmental and occupational exposure to these carbonaceous particles, deeper insight into the (eco-) toxicological impact of these materials is of critical importance.

So far however, no experimental methods have been reported that enable direct detection of carbon black/black carbon in relevant samples such as polluted water and consumer products as well as exposed cells and body fluids. To date, only measurements[9-11] in polluted air (see reference 9 for an overview) such as absorption photometry and laser induced incandescence (LII) have been used to determine particle concentrations or alternatively labeling methods[12-14] have been explored such as the technetium-99-m radionuclide labeling in epidemiological studies and toxicology research.

In LII, the emission from carbonaceous materials has been linked to black-body radiation from the severely heated CB particles,[15] *i.e.* incandescence. Already various models have been proposed to explain the origin of incandescence and its dependence on illumination power and pulse duration.[16-18] Recently, substantial scientific efforts have focused on white light (WL) emission from carbonaceous materials including graphene[19], fullerenes[20] and carbon nanotubes[21]. Also for these materials the emitted radiation has been linked to incandescence. However, visible emission from CB particles in solution and biological matter has so far not been sufficiently explored, despite reports of CB suspensions serving as optical limiters and nonlinear scatterers due to their broadband and flat absorption.[16, 17] The interpretation of these effects is not straightforward as they strongly depend on the experimental conditions.[22] Recently, luminescence of carbon particles has been described but this phenomenon seems to be limited to carbon nano-dots, *i.e.* carbon nanoparticles with sizes below 10 nm.[23, 24]

To the best of our knowledge, we report here for the first time non-incandescence related WL emission of CB particles in aqueous environments under femtosecond pulsed illumination using a multiphoton laser-scanning microscope and demonstrate its potential in a biological context. This label-free approach to directly visualize CB offers additional advantages (schematic representation in Figure 1A) such as inherent 3D sectioning and high imaging depths owing to the multiphoton approach. We anticipate that this method will play an important role in health related studies where the impact and role of CB particles is to be assessed at the organism, tissue, cellular and subcellular level.

In this study a variety of carbonaceous particles, representative for those to which humans are typically exposed, is used ranging from powders used in copy machines to materials that are typically employed as model for soot. Information on the physico-chemical characteristics of these different commercial CB materials (ufPL, ufP90, CCB and fCB) can be found in Table S1 in the supplementary information (SI). According to manufacturer's data, the aerodynamic diameter of the particles varies between 13 and 500 nm. Transmission electron microscopy (TEM) images (Figure 1B and S1) show the typical appearance of CB consisting of aciniform aggregates of primary carbon particles with arbitrary shape. These TEM images and the results from dynamic light scattering summarized in Table S1 show that CB particles aggregate when suspended in aqueous solutions, and absorb corona proteins from the complete medium onto their surface resulting in an increased hydrodynamic diameter and a zeta-potential corresponding to approximately -20 mV regardless of their native potential. In conclusion, the physico-chemical characteristics of the different CB particles in suspension are similar although when selecting the particles we aimed for as much difference as possible.

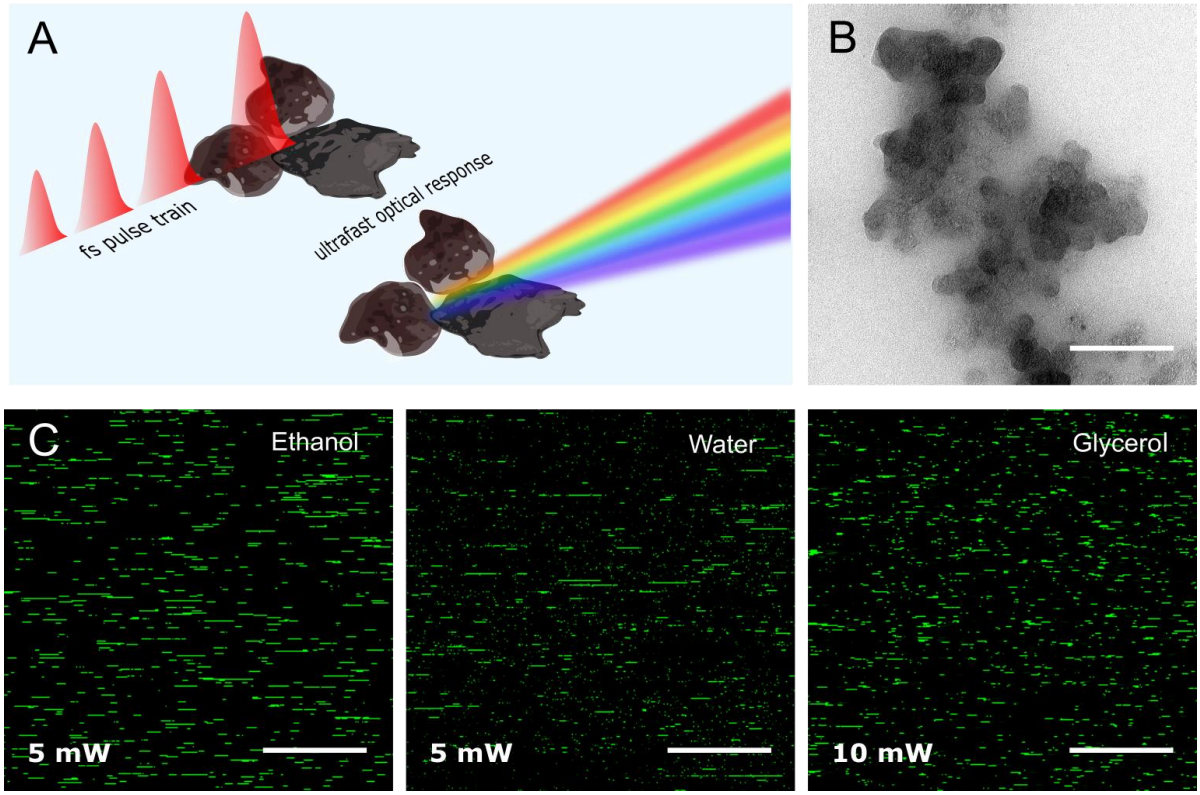

Figure 1. (A) Schematic representation of the illumination and emission process of CB particles for the presented detection method. (B) TEM image of an ufPL aggregate. Scale bar: 300 nm. (C) CCB (600 µg/mL) imaging in ultrapure water, ethanol and glycerol at room temperature upon illumination with 5 or 10 mW average laser power at the sample (excitation 810 nm, 80 MHz). Scale bars: 15 µm. Emission band: 450 – 650 nm.

Figure 1C displays CB suspended in ultrapure water, ethanol and glycerol illuminated with a femtosecond laser at 810 nm (150 fs, 80 MHz) and recorded using a commercial multiphoton laser-scanning microscope (detailed information on sample preparation and microscopy modalities can be found in SI). Intense signals were detected with an emission band pass filter of 450 to 650 nm in front of the detector. Depending on the suspension medium, the laser power needs to be adjusted to generate similar emission intensity: in glycerol and immersion oil the illumination power was about twice that of the experiment in ethanol or water (SI, Figure S2). Note the horizontal smearing of the CB particles in Figure 1C (pixel

111 dwell time of 1.60 µs, pixel size of 220 nm). This phenomenon is observed at all
112 combinations of scan speeds and zooms (data not shown), suggesting susceptibility of the
113 particles to optical trapping under these conditions. This hypothesis is further supported by
114 the absence of this smearing when CB particles are embedded in polydimethylsiloxane
115 (Figure S3). Trapping by femtosecond laser pulses has already been shown for other types of
116 nanoparticles.[25, 26]
117
118 Additional spectroscopic measurements were performed to investigate the observed visible
119 light emission under femtosecond near-infrared illumination.
120
121 Firstly, we rule out photoluminescence (PL) reported for very small carbonaceous particles
122 (below 10 nanometer)[23, 24, 27] as a cause of the observed emission. Carbonaceous particles, in
123 particular soot, consist of aggregated particles that are heterogeneous in nature[28] and
124 therefore contain multiple absorbing species possibly responsible for radiative transitions.
125 The extinction spectra of aqueous suspensions of the CB particles considered here cover the
126 whole visible range (Figure 2A), presumably due to a continuum of electronic states in the
127 amorphous carbon. The slight increase of the extinction towards lower wavelengths for the
128 two smaller particles (ufPL and ufP90) is likely due to increased light scattering.
129

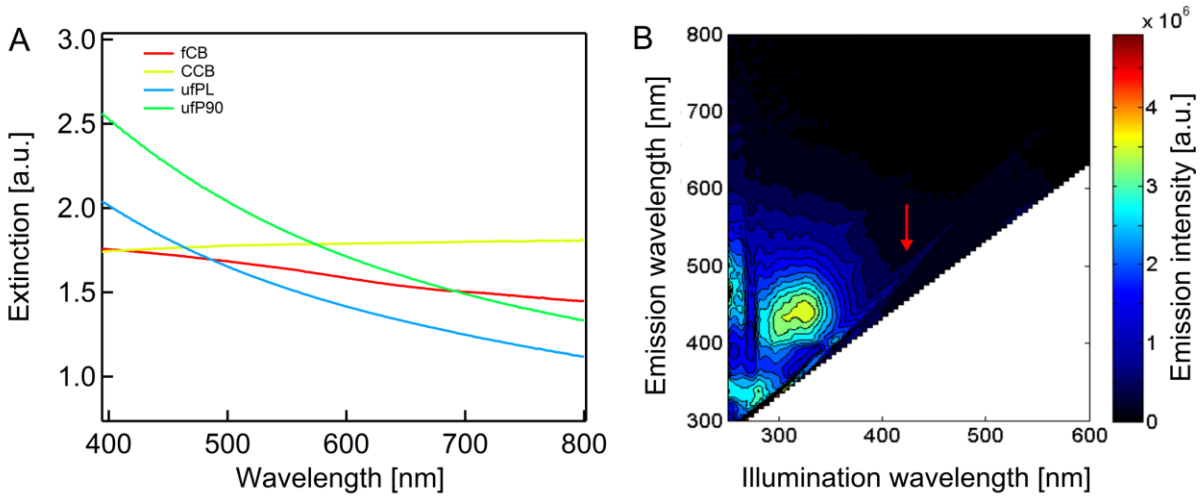

Figure 2. (A) Extinction spectra of aqueous CB suspensions. (B) Two-dimensional excitation-emission plot of ufPL particles in water under single photon excitation with a false color map based on the emission intensity in arbitrary units. The red arrow points towards the Raman line of water.

Two-dimensional single photon excitation-emission plots (Figure 2B) of ufPL (similar plot for fCB: SI, Figure S4) however, show only weak emission; note in comparison the weak Raman line (red arrow) of water, the suspension medium. The luminescence under excitation in the ultraviolet (UV) region (280 – 380 nm) looks similar to the observations described by Kwon *et al.* for carbon nano-dots[29, 30] and hints towards micro-crystalline graphite exhibiting only a low number of tetrahedral sp^3-sites[30-32] which is also confirmed by Raman spectra (SI, Figure S5 and Table S2).

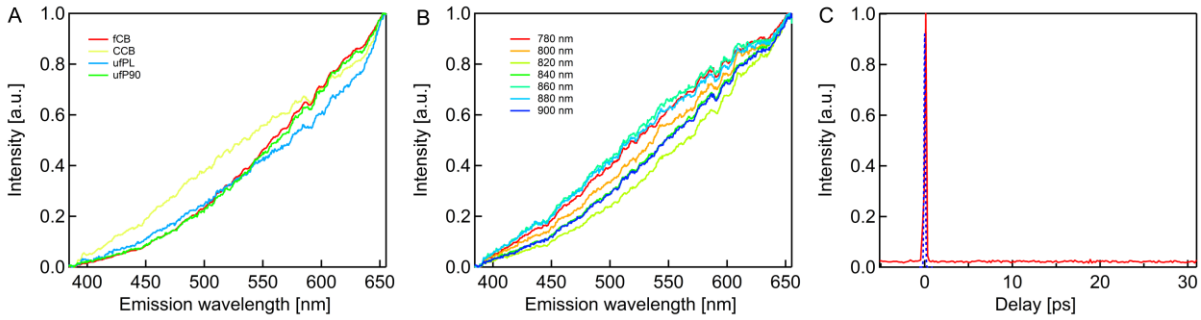

Figure 3. (A) Normalized WL emission spectra of aqueous CB particle suspensions using femtosecond 810 nm laser illumination (8 mW, 150 fs, 80 MHz). (B) Normalized WL emission spectra of aqueous ufP90 suspensions recorded at different femtosecond illumination wavelengths. (C) Temporal response of aqueous carbon suspension measured by femtosecond photoluminescence up-conversion experiments. Also shown is the instrument response function (dashed line).

In contrast to single photon excitation, illumination with femtosecond pulsed near-infrared light (810 nm, 150 fs, 80 MHz) generates a strong, feature-less white light emission stretching the whole visible spectrum (Figure 3A and B). This observation was made for all four types of aqueous CB suspensions used in this study and even for dry particles (SI, Figure S6). This WL emission is independent of the illumination wavelength within the range of 780 to 900 nm for a constant average power of 8 mW at the sample (Figure 3B, see also SI, Figure S7).

While PL as visible in Figure 2B cannot explain the strong WL emission observed under femtosecond illumination (Figure 1C, 3A and B), time-resolved investigations are indicative. Using time correlated single photon equipment, an instantaneous nature of the WL radiation is noticed when looking at the picosecond timescale (SI, Figure S8). Also in femtosecond up-conversion experiments with a higher temporal resolution the emitted signal of the CB

166 particles is witnessed to be instantaneous (Figure 3C). On further note, illumination with 7 ps
167 pulses results in a strongly reduced luminescence intensity (SI, Figure S9). The WL emission
168 from the suspended CB particles is therefore only efficiently triggered by femtosecond
169 illumination with high peak electromagnetic fields and once the femtosecond illumination
170 pulse ceases, the WL emission terminates immediately.
171
172 The instantaneous nature of the observed signal confirms that we are not dealing with
173 incandescence despite using laser illumination with fluences of about 0.05 J/cm² at 0.1 nJ
174 pulse energy, similar to previous experiments. In those reports, the observed incandescence
175 showed clear decay times in the microsecond time scale regime[31] due to the cooling down of
176 the lattice at these time scales. In fact, heating of the particle lattice, which is required for
177 incandescence, only occurs on a picosecond time scale when remaining non-emitted energy
178 will be converted into lattice vibrations.[32-34] The femtosecond illumination employed here is
179 too fast.
180
181 The observed instantaneous WL emission is also not related to local refractive index changes
182 in the CB nanoparticle environment upon pulse arrival. Gold nanoparticles are for example
183 known to form nanometer-sized bubbles when illuminated with pulsed lasers at laser
184 fluencies similar to those applied here.[31, 35] and those have been observed leading to broad
185 featureless WL emission.[35-38] If a related principle would be underlying the observed WL
186 emission in CB suspension, the emission spectra would be strongly influenced by the
187 surrounding refractive index. However, even dry particles show the same spectral profile as
188 those suspended in water (SI, Figure S6).
189

We believe that the observed visible light emission under femtosecond near-infrared illumination is related to the broad anti-Stokes emission with non-linear power dependence that was previously observed by other groups for noble metal nanoparticles. In those experiments, the emission arose from femtosecond illumination of gold and silver particles or nanostructures.[39-42] We can confirm that also the WL emission of CB displays a nonlinear, second order response with respect to the incident power (SI, Figure S10). The WL emission of gold was recently succinctly investigated by Haug *et al.*[43] Here, plasmonic confinement of electric fields in metal along with the small dimensions of the emitting particle can presumably relax symmetry selection and momentum conservation rules to allow for (continuous) intraband dipole transitions, which would otherwise be impossible. The observed emission is independent of the type of metal and the preparation conditions. Even though carbon particles are not metallic in nature and do not show plasmonic modes in the visible or near UV spectral range (see Figure 2A), an electron gas could emerge on arrival of a femtosecond pulse. At very high energies, even plasmons or plasmon-like effects have been discovered with electron energy loss spectroscopy in carbon nanotubes and its parent material graphene[44-46] or in graphitic spheres[47]. Buckminsterfullerene[48] and other carbonaceous materials[49] show strong multiphoton ionization. The intense and spectrally broad absorption of the particles could give rise to this phenomenon, promoting resonant multiphoton transitions leading to ionizations.[50] Therefore, consecutive intraband transitions similar to those noticed in plasmonically active metals could be a valid explanation for the observed results.

As a result of visible WL generation by carbon black particles under femtosecond pulsed near-infrared illumination, the signal of the particles can easily be combined with various conventional contrast-enhancing fluorophores used to visualize biological features. As shown

in Figure 4, the emitted WL can be probed at different wavelengths at laser powers compatible with life cell imaging. Hence, CB detection can be combined with the imaging of cellular compartments stained by different color-label fluorophores (labeling strategy can be found in SI). This simultaneous detection enables unequivocally localization of the particles inside the cells and puts the CB location directly into its biological context.

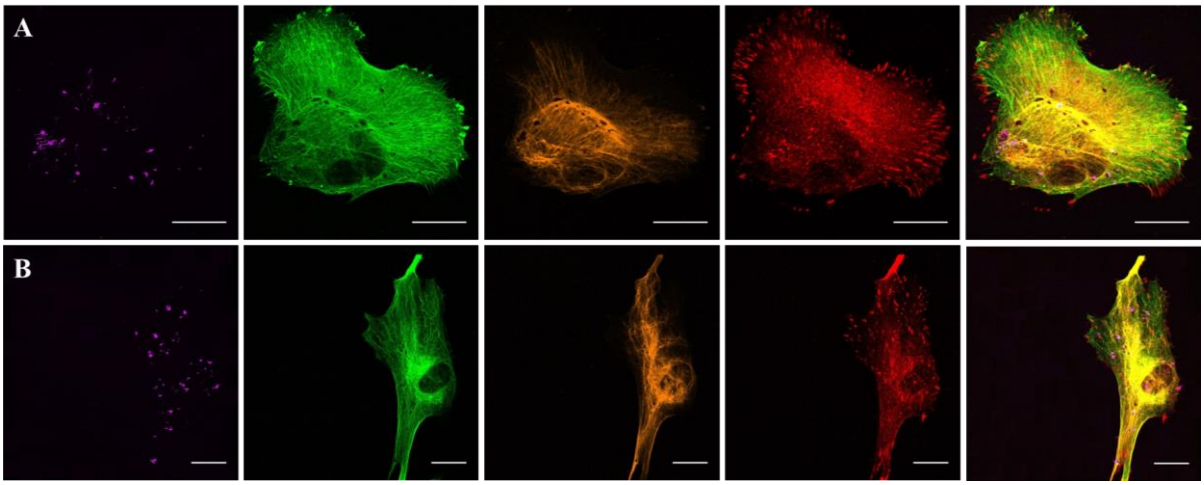

Figure 4. Imaging of cellular compartments of fixed MRC-5 cells stained with commonly utilized fluorophores and in combination with the detection of CCB particles (4 h incubation of 5 µg/cm^2 CCB at 37 °C prior to imaging). Emission of the carbonaceous particles can be probed at different wavelengths, here shown at (A) 400 – 410 nm in the non-descanned mode and (B) 650 – 710 nm in descanned mode (4 mW average laser power at the stage). From left to right: CCB particles, tubulin cytoskeleton (Ex/Em 495/519 nm, ~ 3 µW radiant power at the sample), vimentin which is an intermediate filament protein of the cytoskeleton (Ex/Em 555/565 nm, ~ 3 µW radiant power at the sample), paxillin expressed at focal adhesions (Ex/Em 650/665 nm, ~ 3 µW radiant power at the sample), and overlay image. Scale bars: 25 µm.

233 To further illustrate the versatility of the technique in a biological setting, a co-localization
234 study of the tubulin cytoskeleton of MRC-5 lung fibroblasts and engulfed carbon particles
235 was performed (Figure 5). The images show a clear impact of CCB on the architecture of the
236 tubulin cytoskeleton of the cells for an incubation that exceeds four hours at 37 °C. More
237 specifically, the supporting cytoskeleton network evolves from the commonly observed fiber-
238 like structure to a partial diffuse and holey configuration. The cytoskeletal alteration is also
239 reflected in the overall morphology of the cells. Their appearance changed from the normal
240 bipolar and stretched morphology to a smaller and more irregular shaped one, which is an
241 indication of apoptosis (these biological findings are also true for the other smaller CB
242 particles, for an additional example with ufP90, see SI, Figure S11).[51-53] These images do not
243 only pinpoint the versatility in biological settings but also immediately indicate the social
244 relevance and significance of this detection technique. Potential advantageous information
245 arising from this simultaneous detection comprise the correlations that can be made between
246 the location of the particles and the altered cellular structure (*e.g.,* cytoskeleton and focal
247 adhesions). This makes the observed WL emission an extremely interesting label-free
248 detection mechanism for biomedical research including toxicology and epidemiology.
249

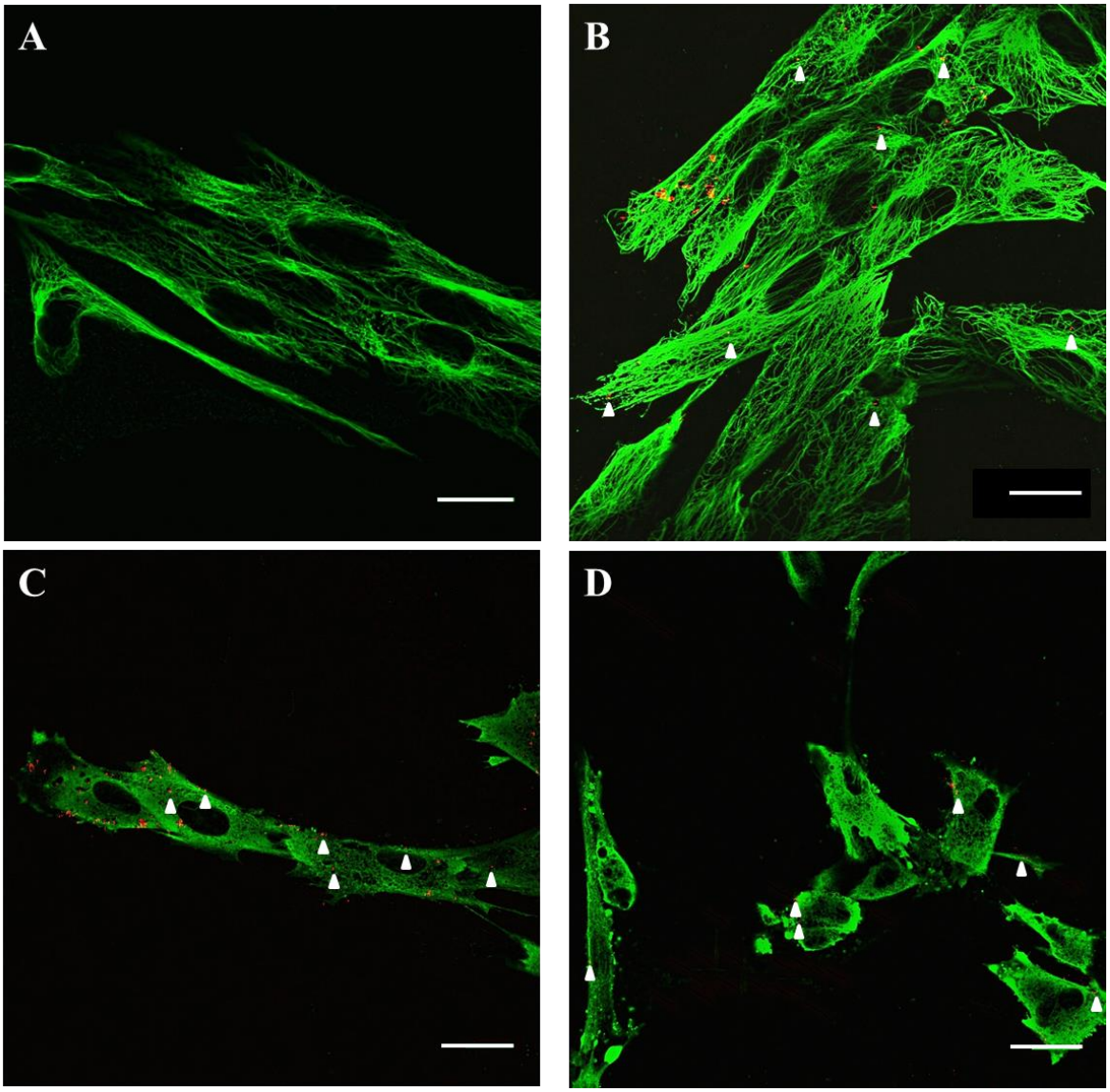

Figure 5. Tubulin cytoskeleton (green, Ex/Em 495/519 nm, ~ 3 µW radiant power at the sample) of normal human lung fibroblasts incubated with 5 µg/cm^2 CCB particles (red, 4 mW average laser power at the sample, emission detection: 400 – 410 nm in non-descanned mode) at 37 °C. (A) Control cells. (B) 4 h incubation. (C) 8 h incubation. (D) 24 h incubation. Scale bars: 30 µm. Arrow heads: some locations of very small, engulfed CCB particles.

To conclude, femtosecond pulsed illumination of CB followed by detection of emitted WL is a straightforward approach without the need of particular sample pretreatment and which can easily be implemented in multiphoton imaging experiments. The nature of the signal makes it very versatile in terms of choice of additional fluorophores. The ease of the reported

approach broadens the potential applicability in the fast growing field of nanotechnology. Additionally, it will advance epidemiological and toxicological studies since this is the first time a technique is described to directly detect carbon black in a biological setting without any additional treatment or labeling required. We anticipate that this technology will make it possible to screen human tissues and body fluids for the presence of CB owing to the multiphoton approach which results in inherent 3D sectioning and high imaging depths. This may eventually lead to valuable information about, for example, the actual uptake and clearance of CB particles by the human body.

ASSOCIATED CONTENT

Supporting Information

Detailed methods and supplemental figures. This material is available free of charge via the Internet at http://pubs.acs.org.

AUTHOR INFORMATION

Corresponding Author

* (M.R.) E-mail: maarten.roeffaers@biw.kuleuven.be. Phone: +3216-327-449.

* (M.A.) E-mail: marcel.ameloot@uhasselt.be. Phone: +3211-269-233.

Author Contributions

‡These authors contributed equally in the performance of the experiments. H.B., C.S., M.R. and M.A. jointly designed and analyzed the experiments. H.B. and C.S. performed most of the experiments. E.F. performed the femtosecond fluorescence up-conversion experiments. E.S. assisted with the time correlated single photon counting. J.D. made the transmission electron microscopy images. H.U. and Y.F. gave their technical support during spectral data collection. M.V. gave theoretical support. The manuscript was written through contributions of all authors. All authors have given approval to the final version of the manuscript.

Notes

The authors declare no competing financial interests. Patent application about the described findings was filed on 12/01/2016 in the UK [patent application number 1600564.7].

Acknowledgements

This research was supported by the Interuniversity Attraction Poles Program (P7/05) initiated by the Belgian Science Policy Office. H.B. acknowledges funding from Research Foundation

Flanders (Fonds Wetenschappelijk Onderzoek, FWO) for a doctoral fellowships: 11ZB115N. C.S. is supported by a postdoctoral FWO fellowship: 12R6315N. The authors also thank FWO for the research grant G082113. M.R. acknowledges financial support from the KU Leuven Research Fund (C14/15/053, OT/12/059). M.A. thanks the Province of Limburg (Belgium) for the financial support within the tUL IMPULS FASE II program, allowing for the upgrading of the laser source used in this work. W. Baekeland is acknowledged for his support with the recording of the single photon extinction and emission spectra. H.B. gratefully acknowledges the assistance of Mrs. P. Bex and Mr. J. Janssen.

REFERENCES

1. ASTM, *American Society for Testing Materials D3053-13a, Standard on Terminology Relating to Carbon Black*. ASTM International: West Conshohocken, PA, 2013.
2. Watson, A. Y.; Valberg, P. A. *AIHAJ* **2001,** 62, (2), 218-228.
3. Castro, L.; Pio, C.; Harrison, R. M.; Smith, D. *Atmos. Environ.* **1999,** 33, (17), 2771-2781.
4. Arnal, C.; Alzueta, M.; Millera, A.; Bilbao, R. *Combust. Sci. Technol.* **2012,** 184, (7-8), 1191-1206.
5. Tankersley, C. G.; Bierman, A.; Rabold, R. *Inhal. Toxicol.* **2007,** 19, (8), 621-9.
6. Bond, T. C.; Bhardwaj, E.; Dong, R.; Jogani, R.; Jung, S.; Roden, C.; Streets, D. G.; Trautmann, N. M. *Glob. Biogeochem. Cycles* **2007,** 21, (2).
7. Lamarque, J.-F.; Bond, T. C.; Eyring, V.; Granier, C.; Heil, A.; Klimont, Z.; Lee, D.; Liousse, C.; Mieville, A.; Owen, B. *Atmos. Chem. Phys.* **2010,** 10, (15), 7017-7039.
8. Wang, R., *Global Emission Inventory and Atmospheric Transport of Black Carbon: Evaluation of the Associated Exposure*. Springer Theses: Beijing, China, 2015.
9. Chow, J. C.; Watson, J. G.; Doraiswamy, P.; Chen, L.-W. A.; Sodeman, D. A.; Lowenthal, D. H.; Park, K.; Arnott, W. P.; Motallebi, N. *Atmos. Res.* **2009,** 93, (4), 874-887.
10. OECD. *Methods of Measuring Air Pollution: Report of the Working Party on Methods of Measuring Air Pollution and Survey Techniques*; Organization for Economic Co-operation and Development: Paris, France, 1964.
11. Schulz, C.; Kock, B. F.; Hofmann, M.; Michelsen, H.; Will, S.; Bougie, B.; Suntz, R.; Smallwood, G. *Appl. Phys. B* **2006,** 83, (3), 333-354.

12. Kong, H.; Zhang, Y.; Li, Y.; Cui, Z.; Xia, K.; Sun, Y.; Zhao, Q.; Zhu, Y. *Int. J. Mol. Sci.* **2013,** 14, (11), 22529-22543.

13. Wang, H.-f.; Troxler, T.; Yeh, A.-g.; Dai, H.-l. *J. Phys. Chem. C* **2007,** 111, (25), 8708-8715.

14. Nemmar, A.; Hoet, P. M.; Vanquickenborne, B.; Dinsdale, D.; Thomeer, M.; Hoylaerts, M.; Vanbilloen, H.; Mortelmans, L.; Nemery, B. *Circulation* **2002,** 105, (4), 411-414.

15. Ferrari, A.; Meyer, J.; Scardaci, V.; Casiraghi, C.; Lazzeri, M.; Mauri, F.; Piscanec, S.; Jiang, D.; Novoselov, K.; Roth, S. *Phys. Rev. Lett.* **2006,** 97, (18), 187401.

16. Belousova, I.; Mironova, N.; Scobelev, A.; Yur'ev, M. *Opt. Commun.* **2004,** 235, (4), 445-452.

17. Zelensky, S. *Semicond. Phys. Quantum Electron. Optoelectron.* **2004,** 7, (2), 190-194.

18. Rulik, J. J.; Mikhailenko, N.; Zelensky, S.; Kolesnik, A. *Semicond. Phys. Quantum Electron. Optoelectron.* **2007,** 10, (2), 6-10.

19. Strek, W.; Cichy, B.; Radosinski, L.; Gluchowski, P.; Marciniak, L.; Lukaszewicz, M.; Hreniak, D. *Light Sci. Appl.* **2015,** 4, (1), e237.

20. Hamilton, B.; Rimmer, J.; Anderson, M.; Leigh, D. *Adv. Mater.* **1993,** 5, (7-8), 583-585.

21. Imholt, T.; Dyke, C. A.; Hasslacher, B.; Pérez, J. M.; Price, D.; Roberts, J. A.; Scott, J.; Wadhawan, A.; Ye, Z.; Tour, J. M. *Chem. Mater.* **2003,** 15, (21), 3969-3970.

22. Fougeanet, F.; Fabre, J.-C. In *Nonlinear mechanisms in carbon-black suspension in a limiting geometry*, MRS Proceedings, 1997; Cambridge Univ. Press: p 293.

23. Li, H.; Kang, Z.; Liu, Y.; Lee, S.-T. *J. Mater. Chem.* **2012,** 22, (46), 24230-24253.

24. Ghosh, S.; Chizhik, A. M.; Karedla, N.; Dekaliuk, M. O.; Gregor, I.; Schuhmann, H.; Seibt, M.; Bodensiek, K.; Schaap, I. A.; Schulz, O. *Nano Lett.* **2014,** 14, (10), 5656-5661.

25. Usman, A.; Chiang, W. Y.; Masuhara, H. *Sci. Prog.* **2013,** 96, (Pt 1), 1-18.

26. Usman, A.; Chiang, W.-Y.; Masuhara, H. In *Femtosecond trapping efficiency enhanced for nano-sized silica spheres*, 2012; pp 845833-845833-7.

27. Li, Q.; Ohulchanskyy, T. Y.; Liu, R.; Koynov, K.; Wu, D.; Best, A.; Kumar, R.; Bonoiu, A.; Prasad, P. N. *J. Phys. Chem. C* **2010,** 114, (28), 12062-12068.

28. Bond, T. C.; Bergstrom, R. W. *Aerosol Sci. Technol.* **2006,** 40, (1), 27-67.

29. Kwon, W.; Do, S.; Kim, J.-H.; Jeong, M. S.; Rhee, S.-W. *Sci. Rep.* **2015,** 5.

30. Carpene, E.; Mancini, E.; Dallera, C.; Schwen, D.; Ronning, C.; De Silvestri, S. *New J. Phys.* **2007,** 9, (11), 404.

31. Michelsen, H. A. *The Journal of chemical physics* **2003,** 118, (15), 7012-7045.

32. Link, S.; El-Sayed, M. A. *J. Phys. Chem. B* **1999,** 103, (40), 8410-8426.

33. Ahmadi, T. S.; Logunov, S. L.; El-Sayed, M. A. *J. Phys. Chem.* **1996,** 100, (20), 8053-8056.

34. Hodak, J.; Martini, I.; Hartland, G. V. *Chem. Phys. Lett.* **1998,** 284, (1), 135-141.

35. Kotaidis, V.; Dahmen, C.; Von Plessen, G.; Springer, F.; Plech, A. *The Journal of chemical physics* **2006,** 124, (18), 184702.

36. Lapotko, D. *Opt. Express* **2009,** 17, (4), 2538-2556.

37. Lapotko, D. *Int. J. Heat Mass Trans.* **2009,** 52, (5), 1540-1543.

38. Lukianova-Hleb, E. Y.; Sassaroli, E.; Jones, A.; Lapotko, D. O. *Langmuir* **2012,** 28, (10), 4858-4866.

369 39. Kim, H.; Sheps, T.; Taggart, D. K.; Collins, P. G.; Penner, R. M.; Potma, E. O. In
370 *Coherent anti-Stokes generation from single nanostructures*, SPIE BiOS: Biomedical
371 Optics, 2009; International Society for Optics and Photonics: pp 718312-718312-8.
372 40. Beversluis, M. R.; Bouhelier, A.; Novotny, L. *Phys. Rev. B* **2003,** 68, (11), 115433.
373 41. Danckwerts, M.; Novotny, L. *Phys. Rev. Lett.* **2007,** 98, (2), 026104.
374 42. Palomba, S.; Danckwerts, M.; Novotny, L. *J. Opt. A-Pure Appl. Op.* **2009,** 11, (11),
375 114030.
376 43. Haug, T.; Klemm, P.; Bange, S.; Lupton, J. M. *Phys. Rev. Lett.* **2015,** 115, (6),
377 067403.
378 44. Kramberger, C.; Hambach, R.; Giorgetti, C.; Rümmeli, M.; Knupfer, M.; Fink, J.;
379 Büchner, B.; Reining, L.; Einarsson, E.; Maruyama, S. *Phys. Rev. Lett.* **2008,** 100,
380 (19), 196803.
381 45. Ajayan, P.; Iijima, S.; Ichihashi, T. *Phys. Rev. B* **1993,** 47, (11), 6859.
382 46. Pichler, T.; Knupfer, M.; Golden, M.; Fink, J.; Rinzler, A.; Smalley, R. *Phys. Rev.*
383 *Lett.* **1998,** 80, (21), 4729.
384 47. Stöckli, T.; Bonard, J.-M.; Châtelain, A.; Wang, Z. L.; Stadelmann, P. *Phys. Rev. B*
385 **1998,** 57, (24), 15599.
386 48. Ding, D.; Compton, R.; Haufler, R.; Klots, C. *J. Phys. Chem.* **1993,** 97, (11), 2500-
387 2504.
388 49. Pratt, S. T.; Dehmer, J. L.; Dehmer, P. M. *J. Chem. Phys.* **1985,** 82, (2), 676-680.
389 50. Streibel, T.; Zimmermann, R. *Annu. Rev. Anal. Chem.* **2014,** 7, 361-381.
390 51. Hussain, S.; Thomassen, L. C.; Ferecatu, I.; Borot, M.-C.; Andreau, K.; Martens, J.
391 A.; Fleury, J.; Baeza-Squiban, A.; Marano, F.; Boland, S. *Part. Fibre Toxicol.* **2010,**
392 7, (1), 1.

393 52. Sydlik, U.; Bierhals, K.; Soufi, M.; Abel, J.; Schins, R. P.; Unfried, K. *Am. J. Physiol.*
394 *Lung Cell. Mol. Physiol.* **2006,** 291, (4), L725-L733.
395 53. Bortner, C.; Cidlowski, J. *Cell Death Differ.* **2002,** 9, (12), 1307-1310.

396